



OPEN ACCESS

EDITED BY

Abbas Khan,
Abdul Wali Khan University Mardan,
Pakistan

REVIEWED BY

Kajal Ghosal,
Jadavpur University, India
Hassan SHah,
The University of Chenab, Pakistan

*CORRESPONDENCE

Kashif Barkat,
✉ kashif.barkat@pharm.uol.edu.pk
Mohammed Bourhia,
✉ bourhiamohammed@gmail.com

RECEIVED 11 July 2023

ACCEPTED 23 October 2023

PUBLISHED 06 November 2023

CITATION

Umar A, Barkat K, Hussain Shah SN, Ashraf MU, Badshah SF, Ali A, Anjum I, Bin Jordan YA, Nafidi H-A, Dauelbait M and Bourhia M (2023), Porous and highly responsive polymeric fabricated nanometrices for solubility enhancement of acyclovir; characterization and toxicological evaluation. *Front. Mater.* 10:1257047. doi: 10.3389/fmats.2023.1257047

COPYRIGHT

© 2023 Umar, Barkat, Hussain Shah, Ashraf, Badshah, Ali, Anjum, Bin Jordan, Nafidi, Dauelbait and Bourhia. This is an open-access article distributed under the terms of the [Creative Commons Attribution License \(CC BY\)](https://creativecommons.org/licenses/by/4.0/). The use, distribution or reproduction in other forums is permitted, provided the original author(s) and the copyright owner(s) are credited and that the original publication in this journal is cited, in accordance with accepted academic practice. No use, distribution or reproduction is permitted which does not comply with these terms.

Porous and highly responsive polymeric fabricated nanometrices for solubility enhancement of acyclovir; characterization and toxicological evaluation

Ayesha Umar¹, Kashif Barkat^{1*}, Syed Nisar Hussain Shah¹, Muhammad Umer Ashraf¹, Syed Faisal Badshah², Akhtar Ali³, Irfan Anjum⁴, Yousef A. Bin Jordan⁵, Hiba-Allah Nafidi⁶, Musaab Dauelbait⁷ and Mohammed Bourhia^{8*}

¹Faculty of Pharmacy, University of Lahore, Lahore, Pakistan, ²Department of Pharmacy, Faculty of Medical and Health Sciences, University of Poonch, Rawalakot, Pakistan, ³Department of Pharmaceutics, Faculty of Pharmaceutical Sciences, Government College University Faisalabad, Faisalabad, Punjab, Pakistan, ⁴Department of Basic Medical Sciences, Shifa College of Pharmaceutical Sciences, Shifa Tameer-e-Millat University, Islamabad, Pakistan, ⁵Department of Pharmaceutics, College of Pharmacy, King Saud University, Riyadh, Saudi Arabia, ⁶Department of Food Science, Faculty of Agricultural and Food Sciences, Laval University, Quebec City, Canada, ⁷Department of Scientific Translation, Faculty of Translation, University of Bahri, Khartoum, Sudan, ⁸Department of Chemistry and Biochemistry, Faculty of Medicine and Pharmacy, Ibn Zohr University, Laayoune, Morocco

Solubility is one of the major factors which affects several therapeutic moieties in terms of their therapeutic efficacy. In the current study, we presented a porous and amorphous nanometrices system for the enhancement of the solubility of acyclovir. The polymeric network was fabricated by crosslinking polyethylene glycol-6000, polycaprolactone, and β -cyclodextrin with methacrylic acid by optimizing free radical polymerization technique using methylene bisacrylamide as a crosslinking agent. The formulated nanometrices were then characterized by zetasizer, FTIR, PXRD, Scanning electron microscopy, Thermogravimetric analysis, swelling, sol-gel fraction, drug loading, stability, solubility, and *in-vitro* dissolution analysis. Since the formulated system has to be administered orally, therefore to determine the *in-vivo* biocompatibility, nanometrices were administered orally to experimental animals. SEM images provided a rough and porous structure while PXRD showed an amorphous diffractogram of the unloaded and loaded nanometrices. Moreover, the particle size of the optimum loaded formulation was 25 nm higher than unloaded nanometrices due to the repulsion of the loaded drug. A significant loading of the drug with enhanced solubility and dissolution profiles was observed for the poorly soluble drug. The dissolution profile was quite satisfactory as compared to the marketed brand of drug which depicted that the solubility of the drug has been enhanced. Toxicity study conducted on rabbits confirmed the biocompatibility of the nanometrices. The systematic method of preparation,

enhanced solubility and high dissolution profile of the formulated nanometrices may be proved as a promising technique to enhance the solubility of poorly aqueous soluble therapeutic agents.

KEYWORDS

solubility, nanometrices, acyclovir, thermal analysis, toxicity studies

1 Introduction

In order to achieve optimal therapeutic efficacy, it is essential that drugs must possess enhanced bioavailability. The bioavailability of certain drugs is constrained due to factors such as their water solubility, significant first-pass metabolism, and reflux (Fernandes et al., 2018). Oral route remains the most preferable route for administration of drugs (Ghosal et al., 2020). The effectiveness of orally taken drugs is primarily dependent upon their solubility and permeability. The absorption of the drugs from the gastrointestinal tract (GIT) is impeded by two factors including limited solubility in water and low permeability. In order to attain optimal treatment outcomes and obtain maximum plasma concentration, it is typical to deliver drugs at high doses (Homayun et al., 2019; Zhou et al., 2019; Chivere et al., 2020). Limited solubility, permeability, and high first-pass effect are the challenging factors in the development and formulation design process (Martinez and Amidon, 2002; Hua, 2020). Currently, many newly developed drugs that are in the process of being development are facing the issue of having low solubility in water (Jermain et al., 2018; Sharma et al., 2019). As per literature, 40% of the drug that are available in the market are suffering from poorly aqueous solubility while an estimated 70%–90% of drugs that are during research and development are also having the same issue (Xie and Yao, 2018; Dong and Hadinoto, 2019). Poorly aqueous soluble drugs have limited solubility, bioavailability and diminished therapeutics affects and because of these factors, such drugs are being moved from GIT before their maximum dissolution is achieved and hence no beneficial affects are obtained (Xie and Yao, 2018). Nanometrices are three-dimensional, physically and chemically crosslinked nanosized polymeric networks. They have a significant ability to encapsulate drugs inside their polymeric network, increased colloidal stability, high water content, and ease of surface modification. Owing to the above-mentioned properties, nanometrices have gained greater attention as compared to other drug delivery systems. Through self-assembly processes like Van der Waals, electrostatic contacts, and/or hydrophobic interactions between the drug molecules and the polymer, they can load large number of drugs. Such systems can be administered easily and have the swelling capacity of 1–30 times of its original three-dimensional structure. Due to their nanoscale structure, nanometrices have the ability to improve the solubility and pharmacokinetics of the loaded therapeutic agents. Nanometrices possess notable attributes that render them highly promising for utilization in drug delivery systems, as they exhibit the ability to regulate both drug release and pharmacokinetic features (Badshah et al., 2021). They can be delivered orally, nasally, parenterally, topically, or intravenously and have the ability to encapsulate both hydrophilic and hydrophilic drugs (Khan et al., 2022a). Polyethylene glycol-6000 (PEG-6000) is a natural polymer having a molecular weight of 6,000 g/mol. It is a hydrophilic and

nonionic polymer (Ahmad et al., 2020). It has good biocompatibility and can be used in several delivery systems (Tan et al., 2022). Polycaprolactone (PCL) is a bioresorbable polymer and has been widely used for a very long time because of having significant applications in tissue engineering and drug delivery. Polycaprolactone (PCL) has very desirable attributes such as favorable cytocompatibility, non-toxic nature, appropriate mechanical qualities, and a distinctive degradation pattern lasting for a duration of up to 2 years. The extended drug release profile of this polymer exhibits a duration that extends beyond several months. The compound exhibits increased solubility in various organic solvents, leading to its extensive utilization in the development of nanospheres, nanoparticles, fibers, and foams, owing to its exceptional solubility properties (Altun et al., 2022). β -CD, a low-cost polymer, is a highly satisfactory biocompatible polymer. With no toxicity, it has significant aqueous solubility and extensive entrapment efficiency. Structurally, it is a cyclic oligosaccharide, made up of seven dextrose units with a hydrophobic interior and a hydrophilic outside. The structural configuration of β -CD make it a suitable candidate for enhanced loading, swelling, reinforcing, and delaying component release (Uyanga et al., 2020). Acyclovir (ACV) is classified as a synthetic purine nucleotide due to the presence of an aliphatic functional group on its side chain. The mechanism of action of this compound is demonstrated by its ability to hinder the reproduction process of the virus by competitive inhibition of the synthesis of viral DNA. ACV is a poorly aqueous soluble drug and has a limited solubility of 1.2 mg mL^{-1} . At higher doses (800 mg), it is placed in BCS-IV drugs. It has a bioavailability of 10%–30%, and about 70%–90% of the administered drug is eliminated from the body without showing any therapeutic activity. Both poor solubility and less permeability characteristics add to the less oral bioavailability of the drug. For maximum therapeutic effects, an oral dose of 200 mg is administered five times a day. Limited solubility is a main concern for several drugs since such drugs are eliminated from GIT before their dissolution, adding in reduced bioavailability and therapeutic outcomes (Asghar et al., 2021). Mahmood et al. formulated microparticles to enhance the solubility of acyclovir (Mahmood et al., 2016a). Nair et al. developed inclusion complex of β -CD to enhance solubility of acyclovir (Nair et al., 2014). Asghar et al. fabricated nanospheres to enhance the aqueous solubility of acyclovir (Asghar et al., 2021). Till now, various strategies have been employed to enhance the solubility of poorly aqueous soluble drugs belonging to classes BCS-II and BCS-IV. The strategies employed for solubility enhancement include micronization, supercritical fluid (SCF) process, cyclodextrins complexes, nanocrystals, nanogels/nanometrices, nanoparticles, nano-capsule, micro-particles, liposomes, salt formation, amorphous solid dispersions, nanosuspension, self-emulsifying drug delivery system (SEDDS), polymeric microneedles, micelles, and dendrimers (Khan et al.,

2022b). Among the aforementioned strategies, nanogels/nanometrices have gained much importance and have attracted researchers for their utilization in solubility and permeability enhancement. In current project, nanometrices have been optimized to enhance the solubility of ACV. Nanometrices were formulated by free radical polymerization technique. Varying concentrations of polymers, monomer and crosslinker were used to formulate various sets of nanometrices. The formulated nanometrices were then subjected to several structural and *in-vitro* characterizations. The synthesized drug delivery system have demonstrated potential advantages over the previously reported drug delivery systems in terms of solubility, dissolution, crystallinity, and resources for manufacturing.

2 Materials and methods

2.1 Materials

Acyclovir (ACV) was obtained as a generous gift from Brooks Pharmaceuticals (Pvt) Ltd. Karachi, Pakistan. Poly Ethylene Glycol-6000 (PEG-6000), Polycaprolactone (PCL), β -Cyclodextrin (β -CD), and Methacrylic Acid (MAA) were obtained from Sigma Aldrich Chemie GmbH, Steinheim, Germany. Sodium hydroxide, Potassium chloride, Ammonium persulfate (APS), Methylene bisacrylamide (MBA), Potassium dihydrogen phosphate and hydrochloric acid were acquired from MERCK, Germany. BDH Laboratory Supplies Poole, England supplied the required quantity of ethanol. Distilled water was obtained from postgraduate research laboratory, Faculty of Pharmacy, The University of Lahore, Pakistan.

2.2 Methods

2.2.1 Synthesis of nanometrices

The optimization of free radical polymerization approach was employed to process the synthesis of nanometrices. The polymerization process was initiated within a flask of a spherical shape, which was linked to a condenser. Multiple beakers were selected and precise amounts of polyethylene glycol (PEG), polycaprolactone (PCL), and β -cyclodextrin (β -CD) were added to each beaker. 5 mL of water was added to each beaker containing PEG, PCL and β -CD. Beakers were placed on magnetic stirrers and stirring was processed at 300 rpm maintaining the temperature of 50°C until the polymers were completely dissolved. After complete dissolution, the solubilized polymers were mixed and stirring was continued. A weighed amount of MAA was added to the above mixture followed by the addition of a weighed amount of ammonium persulfate APS solution (solubilized in 1 mL of water) to initiate the polymerization reaction. Cross-linker (MBA), of the required quantity was taken in a beaker having 10 mL of water and was stirred on a magnetic stirrer until a clear solution was obtained. Following a 10 min period of stirring, a transparent solution including polymers, monomer, and initiator was gradually introduced into the cross-linker solution while maintaining a consistent stirring speed. Following a period of uninterrupted stirring lasting 5 min, the mixture was subsequently transferred into a round bottom flask while

undergoing continuous sonication. To eliminate any dissolved oxygen within the mixture, the flask was purged with nitrogen gas and subjected to vortexing using the MS2- Minishaker IKA. The round bottom flask with respective mixture was equipped with a condenser. Subsequently, the flask was immersed in a water bath (specifically, a Memmert water bath) at a temperature of 85°C for a duration of 4–5 h. After the required hours, a gel-like mass was obtained which was washed with a mixture of ethanol and water (50 mL) prepared in a ratio of 1:1 to remove any unreacted surface material. The washed gel was then passed through a sieve (#80) to obtain uniform nanometrices. Uniform-sized nanometrices were then placed in an oven (Memmert) at 40°C to dry for the entire night. During fabrication, the varying ratio of polymers, monomer, and crosslinker were used with a constant ratio of the initiator. Concentrations of used ingredients have been shown in Table 1.

2.3 Characterization

2.3.1 Visual examination

Visual examination was carried out to study the physical appearance of the formulated nanometrices.

2.3.2 Fourier transform infrared spectroscopy (FTIR)

FTIR studies were carried out to determine the presence of respective functional groups both in active ingredients and formulated nanometrices. FTIR studies of ACV, PCL, PEG, β -CD, MAA, unloaded and loaded formulations were carried out. Samples were analyzed by attenuated total reflectance (ATR) Bruker FTIR (tensor 27 series, Ettlingen, Germany). Before examining any samples, an empty cell plate scan was performed, following individual placement of the solid samples on the pike miracle cell covering the zinc selenide (ZnSe) crystal surface and rotation of the assembly to create a compact mass, the samples were scanned using ATR-FTIR (Attenuated Total Reflectance-Fourier Transform Infrared) spectroscopy in the 4,000–650 cm^{-1} range.

2.3.3 Particle size analysis

A particle size analyzer (Malvern zeta sizer nano zs, UK) was used to determine the particle size of the optimized formulation. Particle size, zeta potential, and polydispersibility index of optimized formulation were found out. Water that had been filtered and made ultra-pure was used to suspend nanometrices in it. After eliminating any air bubbles, the prepared sample was added to the appropriate cuvette cell. Data was then acquired after inserting the cuvette cell into the instrument. Zeta sizer used Dynamic Light Scattering (DLS) to first measure the Brownian motion of the particles in the sample and then extrapolated a size from this using well-known theories to determine the sample's size.

2.3.4 Powder X-ray diffraction (PXRD)

The powder X-ray diffraction (PXRD) analysis was accomplished to determine the structural parameters of characteristic moieties and whether the corresponding moieties are crystalline or amorphous. Crystalline and amorphous forms impact the solubility profile of the drug and other moieties. Wide-angle X-ray diffraction patterns of ACV, PCL, PEG, placebo

TABLE 1 Quantities of the polymers, monomer, crosslinker and initiator employed in the fabrication of nanometrices.

Formulations	Polymers PCL/PEG/ β -CD (g)	Monomer MAA (g)	Cross linker MBA (g)	Initiator APS (g)	Solvent (mL)
NMT-1	0.1/0.1/0.1	5	1	0.1	26
NMT-2	0.2/0.2/0.2	5	1	0.1	26
NMT-3	0.3/0.3/0.3	5	1	0.1	26
NMT-4	0.2/0.2/0.2	5	1	0.1	26
NMT-5	0.2/0.2/0.2	6	1	0.1	26
NMT-6	0.2/0.2/0.2	7	1	0.1	26
NMT-7	0.2/0.2/0.2	5	1	0.1	26
NMT-8	0.2/0.2/0.2	5	1.15	0.1	26
NMT-9	0.2/0.2/0.2	5	1.25	0.1	26

Since, we have used varying concentrations of polymers, monomer and crosslinker, therefore, in order to specify the changes in concentrations of respective components, we have made their concentrations in bold. Moreover, the bold NMT is the terminology used to specify nanometrices.



FIGURE 1
Physical appearance of the fabricated nanometrices.

TABLE 2 Particle sizes, zeta potential, and polydispersity indexes of placebo and nanometrices with the loaded drug.

Formulations	Unloaded nanometrices (nm)	Loaded nanometrices (nm)	Zeta potential (mV)	PDI
NMT-1	191.22 \pm 6.05	216.21 \pm 5.67	-31.57 \pm 3.22	0.354
NMT-2	198.15 \pm 6.02	223.19 \pm 5.98	-30.65 \pm 2.98	0.376
NMT-3	215.32 \pm 4.19	240.43 \pm 3.93	-30.54 \pm 3.20	0.397
NMT-4	198.15 \pm 6.02	223.19 \pm 5.98	-30.65 \pm 2.98	0.376
NMT-5	221.60 \pm 4.07	246.30 \pm 3.91	-32.67 \pm 3.24	0.390
NMT-6	237.53 \pm 7.32	262.63 \pm 7.11	-32.91 \pm 5.21	0.410
NMT-7	198.15 \pm 6.02	223.19 \pm 5.98	-30.65 \pm 2.98	0.376
NMT-8	179.29 \pm 3.25	204.33 \pm 3.48	-29.33 \pm 3.69	0.238
NMT-9	176.32 \pm 4.33	201.59 \pm 4.98	-28.63 \pm 4.22	0.220

The bold NMT is the terminology used to specify nanometrices.

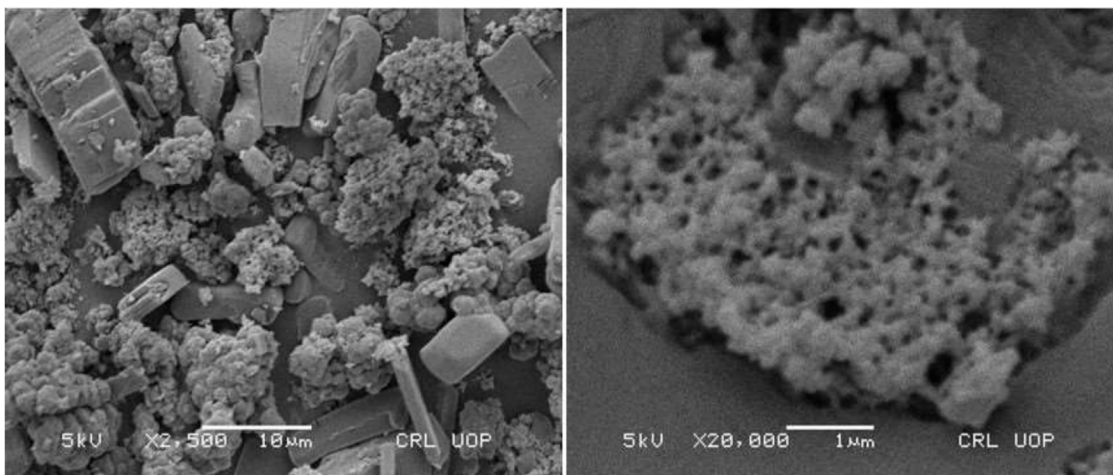


FIGURE 2
SEM images of optimized formulation at various resolution.

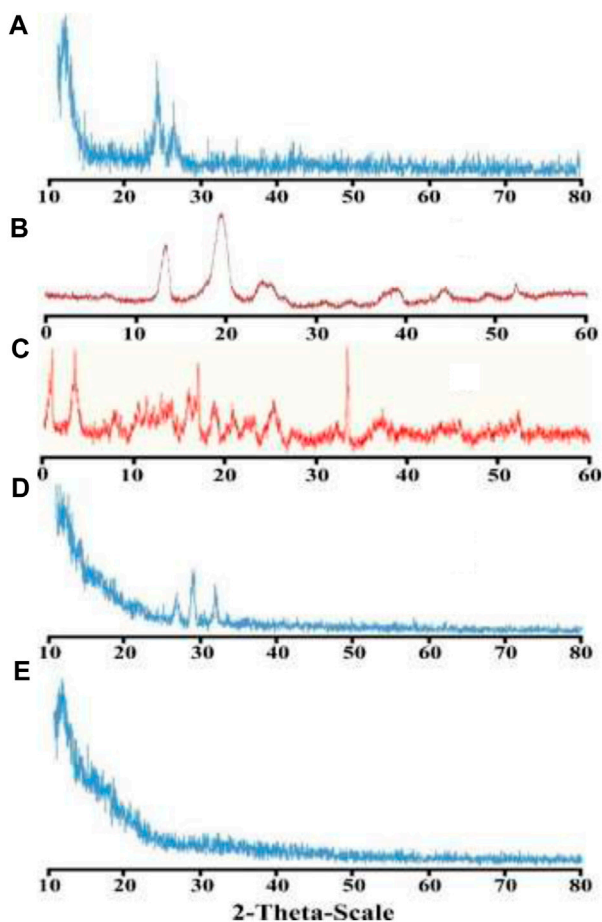


FIGURE 3
Powder X-Ray diffractogram of PCL (A), PEG-6000 (B), β-CD (C), ACV (D), and drug-loaded nanometrices (E).

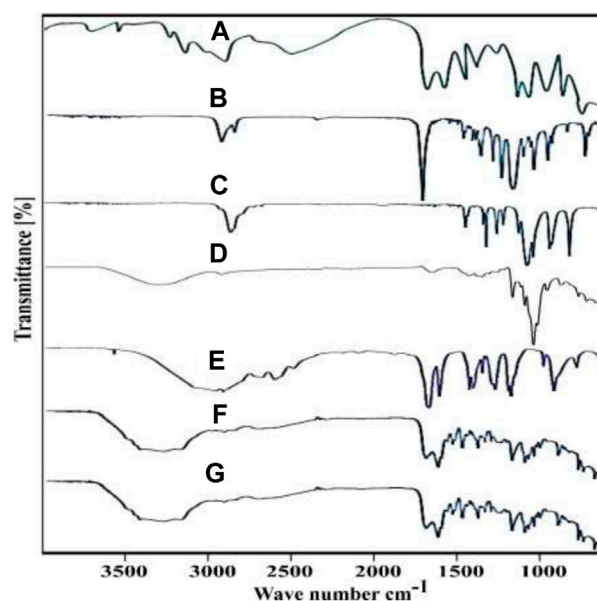


FIGURE 4
FTIR spectra of ACV (A), PCL (B), PEG-6000 (C), β-CD (D), MAA (E), unloaded and loaded nanometrices (F, G).

nanometrices and drug-loaded nanometrices were recorded. The sample holder was loaded with dried powdered nanometrices and peaks were recorded to determine the crystalline or amorphous nature of the corresponding moieties. The range for the PXRD analysis was 0°–60° at a speed of 5°/min.

2.3.5 Thermal analysis

Thermal analyses of drug, polymers, and of optimized nanometrices were performed to assess the stability of

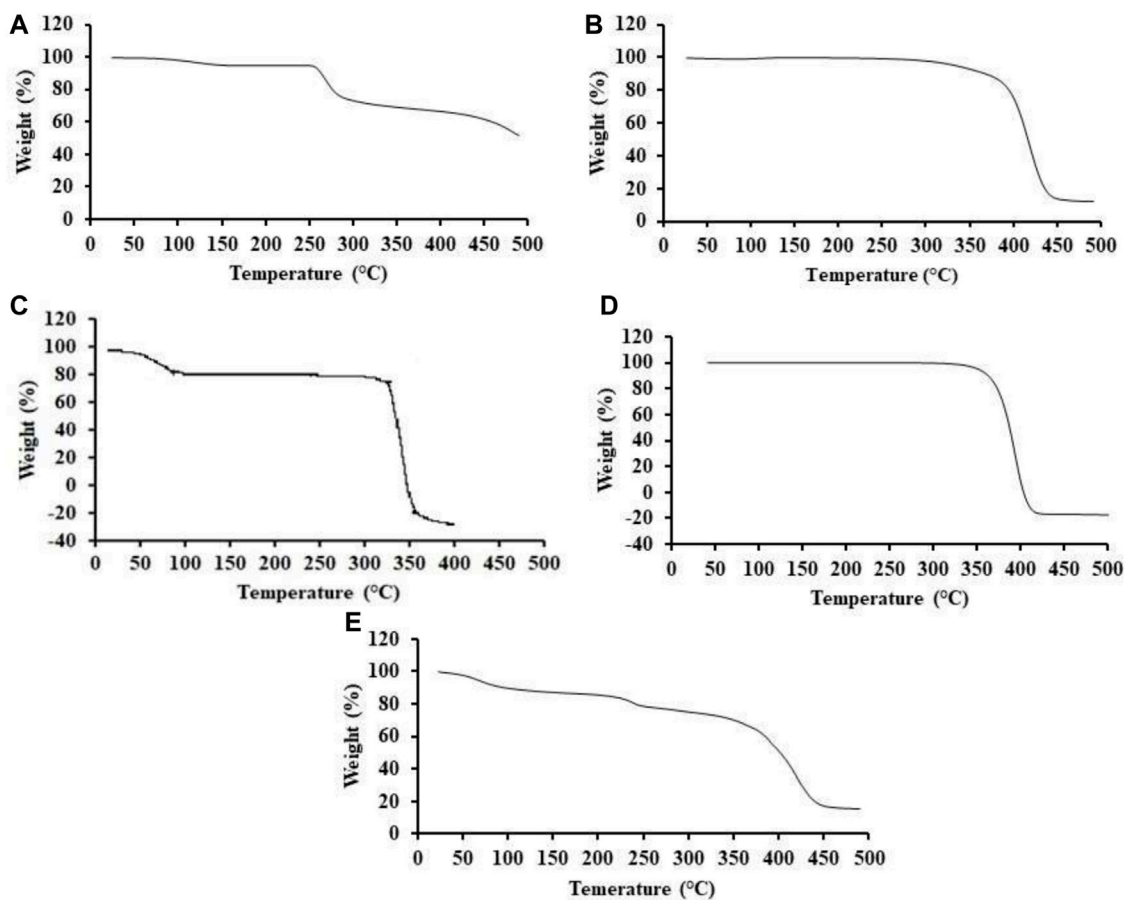


FIGURE 5 TGA thermograms of ACV (A), PEG-6000 (B), PCL (C), β-CD (D) and drug loaded nanometrices (E).

TABLE 3 Sol fraction, gel fraction and percent drug loading of nanomatrices.

S.NO	Formulations	Percent drug loading	Sol fraction	Gel fraction
1	NMT-1	73.291	22.465	77.535
2	NMT-2	75.213	19.406	80.594
3	NMT-3	76.132	21.713	78.287
4	NMT-4	75.213	19.406	80.594
5	NMT-5	79.012	11.508	88.492
6	NMT-6	82.115	8.515	91.485
7	NMT-7	75.213	19.406	80.594
8	NMT-8	71.435	25.545	74.455
9	NMT-9	70.912	26.441	73.559

The bold NMT is the terminology used to specify nanometrices.

optimized formulation. A specific temperature range was adjusted to obtain TGA thermograms of ACV, polymers, and synthesized drug loaded formulation. TGA analysis of

the sample (0.5–5 mg) was carried out at a temperature range of 600 °C with heating at 20 °C/min under a dynamic nitrogen atmosphere.

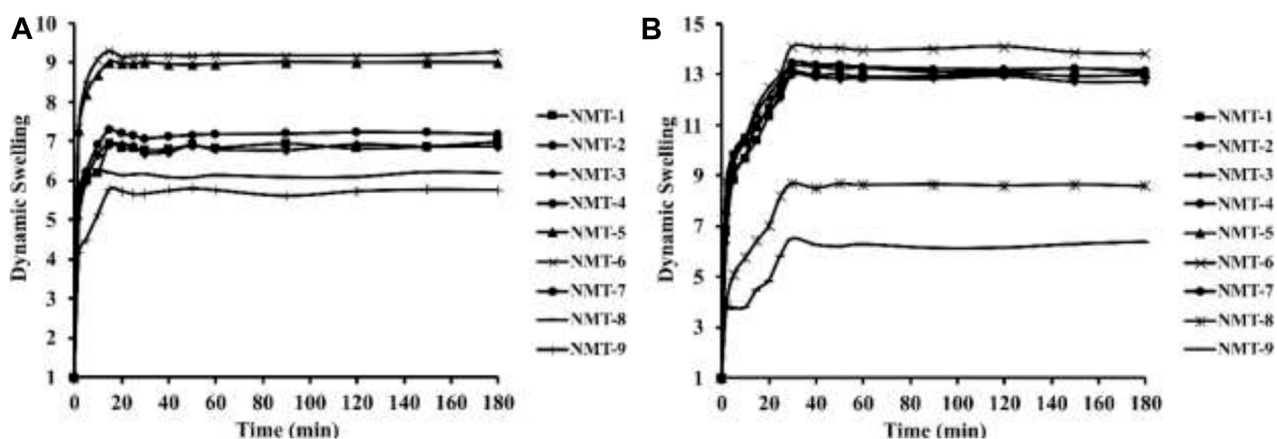


FIGURE 6 Swelling behavior of nanometrices in the swelling media of pH 1.2 (A) and pH 6.8 (B).

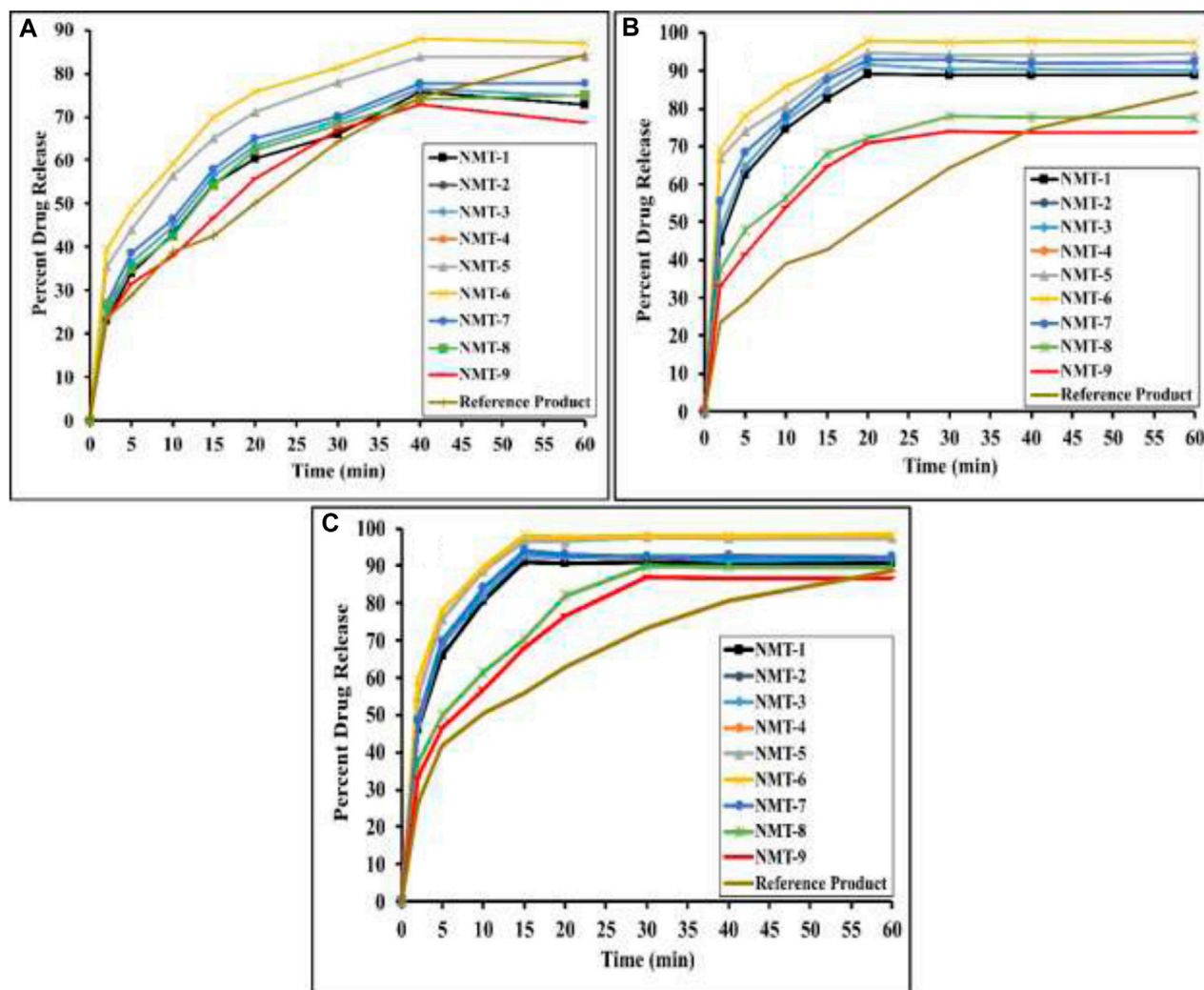


FIGURE 7 *In-vitro* release profile of various formulations and marketed brand in pH 1.2 (A), pH 6.8 (B) and in aqueous medium (C).

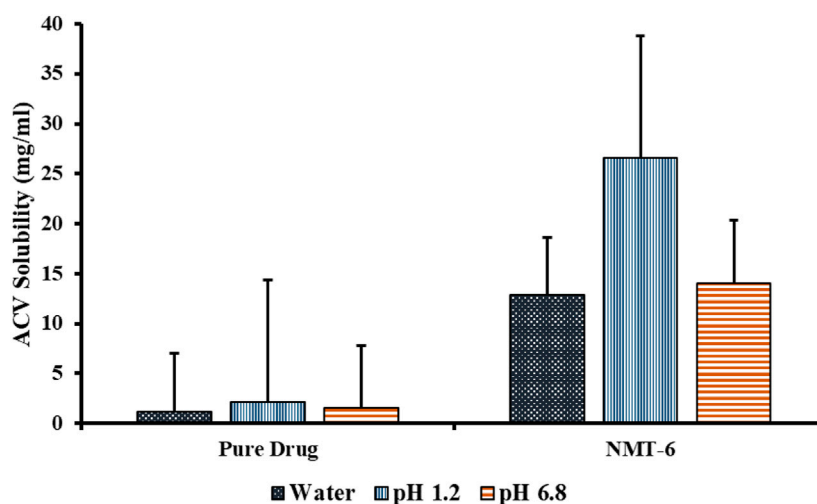


FIGURE 8

Solubility profiles of ACV and optimized formulation in aqueous media and in buffers of pH 1.2 and pH 6.8.

TABLE 4 Stability evaluations of the NMT-6 formulation.

Sr.No	Parameters	0 months	3rd month	6th month
1	Physical appearance	Initially white in color	No significant change	No significant change
2	FTIR spectra	Performed	No prominent change	No prominent change
3	Percent drug loading	85.217%	84.931%	83.592%
4	Swelling ability	Remained constant	No observable change	No observable change

2.3.6 Scanning electron microscopy (SEM)

For determination of surface morphology and porous structure, scanning electron microscopy was carried out (Ghosal et al., 2014). Various resolutions were used to capture images of nanometrices. The samples were thoroughly dried before being mounted on carbon adhesive tape fixed on an aluminum counterfoil. The dried optimized sample was coated with gold for 2 minutes at a rate of 20 mA and was then analyzed under an electron microscope.

2.3.7 Sol-gel fraction

Some of the components used in the formulation of the nanometrices may remain unreacted and their estimation is of prime importance. For this purpose, sol-gel fraction was performed to determine the degree of a chemical reaction. 500 mg of the dried nanometrices without being processed through any treatment was weighed (W_1). For the conduction of sol-gel fraction, samples were placed in the round bottom flask, deionized water of 50 mL was poured into it and a condenser was fitted into its mouth. The Soxhlet extraction technique was employed to perform the sol-gel fraction process. Round bottom flask along with the condenser loaded with nanometrices and 50 mL of deionized water was placed in the waterbath, the temperature of which was already set at 90 °C. The process was carried out for about 5–6 h. After the specified time, nanometrices were removed from the

round bottom flask. In order to achieve a constant weight, nanometrices were first dried in the air and then dried at 40 °C for 24–72 h in an oven. Following thorough drying, nanometrices were weighed once again (W_2), and the sol fraction of dried nanometrices was calculated by subtracting the final weight (W_2) of the nanometrices from the initial weight (W_1). Based on the results of the sol fraction, the gel fraction was calculated. Sol and gel fractions were calculated using the equations below.

$$\text{Sol fraction \%} = \left[\frac{W_1 - W_2}{W_2} \right] \times 100 \quad (1)$$

$$\text{Gel fraction} = 100 - \text{Sol fraction} \quad (2)$$

2.3.8 Swelling studies

In order to evaluate the influence of different media on the swelling of nanometrices over different time intervals (t), a dynamic swelling studies were performed. Dialysis membrane was used for conduction of the swelling studies. The selection of a dialysis membrane was based on its resemblance to a biological membrane. Dialysis membranes containing 100 mg of nanometrices were placed in the corresponding pH 1.2 and 6.8 fluids and allowed to swell. At predefined intervals of 2, 5, 10, 15, 20, 25, 30, 40, 50, 60, 90, 120, 150, 180 min, the medium-immersed dialysis membranes were removed, weighed after being

TABLE 5 Clinical findings of an acute oral toxicity study of optimized nanometrices (NMT-6).

Observation	Group I (control)	Group II (treated with
Signs of illness	Nil	Nil
Body weight (kg)		
Pretreatment	2.15 ± 0.05	2.06 ± 0.05
Day 1	2.18 ± 0.04	2.08 ± 0.04
Day 7	2.25 ± 0.03	2.05 ± 0.05
Day 14	2.27 ± 0.02	2.09 ± 0.07
Water intake (mL)		
Pretreatment	190.30 ± 1.56	193.88 ± 3.70
Day 1	195.31 ± 3.05	190.61 ± 3.85
Day 7	200.45 ± 2.51	196.23 ± 4.90
Day 14	203.12 ± 1.95	200.33 ± 1.50
Food intake (g)		
Pretreatment	72.12 ± 5.13	74.16 ± 3.99
Day 1	73.62 ± 3.52	73.54 ± 3.45
Day 7	74.18 ± 2.12	72.61 ± 3.56
Day 14	73.16 ± 3.70	75.31 ± 4.20
Dermal toxicity: Dermal irritation	Nil	Nil
Ocular toxicity: Simple irritation or corrosion	Nil	Nil
Mortality	Nil	Nil

TABLE 6 Effects of oral administration of optimized nanometrices (NMT-6) on organ weight of rabbits.

Treatment	Heart (g)	Liver (g)	Lung (g)	Kidney (g)	Stomach (g)
Group I (control)	4.38 ± 0.05	74.08 ± 2.61	9.51 ± 0.21	12.8 ± 0.95	12.23 ± 0.71
Group II (test)	4.23 ± 0.07	70.61 ± 3.2	9.7 ± 0.35	12.5 ± 0.95	12.51 ± 0.61

TABLE 7 Biochemical analysis of rabbits' blood treated with blank nanometrices (NMT-6).

Hematology	Group I	Group II (treated with optimized nanometrices
Hemoglobin (g/dL)	12.61 ± 0.45	12.69 ± 1.58
pH	7.14 ± 0.04	7.12 ± 0.41
White blood cells (3109 L21)	6.74 ± 0.48	7.14 ± 0.41
Red blood cells (3,106 mm23)	6.59 ± 0.25	6.03 ± 0.45
Platelets (3109 L21)	4.14 ± 0.28	4.69 ± 0.19
Monocytes (%)	3.23 ± 0.35	3.43 ± 0.22
Neutrophils (%)	55.38 ± 2.09	56.73 ± 2.09
Lymphocytes (%)	65.89 ± 3.98	63.88 ± 2.87
Mean corpuscular volume (%)	65.23 ± 2.12	61.70 ± 3.45
Mean corpuscular hemoglobin (pg/cell)	24.8 ± 0.60	23.72 ± 0.70
Mean corpuscular hemoglobin concentration (%)	30.8 ± 1.02	33.51 ± 1.38

TABLE 8 Liver, kidney and lipid profiles of biochemical analysis rabbits in control and nanometrices treated group.

Biochemical analysis	Group I (control)	Group II (treated with optimized nanometrices)
Alanine aminotransferase (IU/L)	160.61 ± 6.05	165.00 ± 12.0
Aspartate aminotransferase (IU/L)	62.00 ± 3.58	83.31 ± 6.80
Creatinine (mg/dL)	1.19 ± 0.19	1.13 ± 0.25
Urea (mmol/L) 5	13.81 ± 0.54	15.20 ± 2.10
Uric acid (mg/dL)	3.25 ± 0.01	3.15 ± 0.10
Cholesterol (mg/dL)	68.99 ± 6.50	63.32 ± 7.50
Triglycerides (mg/dL)	55.31 ± 7.23	65.00 ± 3.0

blotted with Whatmann's filter paper, and then immersed again in the corresponding media. Following equation was used to determine dynamic swelling (q).

$$q = W_2/W_1 \quad (3)$$

In the above equation, W_1 defines the initial weight while W_2 specifies the final weight of nanometrices after a specific time interval.

2.3.9 Percent drug loading

500 mg of nanometrices were added to the beaker having the dissolved drug (2% drug solution), which was then left at room temperature for 24 h. Since methanol was used along with water for making drug solution, therefore, to thoroughly remove the methanol, drug-loaded nanometrices were dried at 40 °C for 2 hours in the oven. After 2 h, nanometrices with the loaded drug were lyophilized to eliminate any retained solvent. The following formula was used to determine the drug's percent loading.

$$\text{Drug loading (\%)} = \left[\frac{W_D - W_d}{W_d} \right] \times 100 \quad (4)$$

In the above Eq 4, W_d and W_D are the weights of dried nanometrices before and after immersion in the drug solution.

2.3.10 *In vitro* release study

The *in-vitro* release studies of the developed nanometrices and the commercially available tablet were conducted using a calibrated six-station dissolution test apparatus with USP type-2 apparatus paddles. Each dissolution medium, including phosphate buffer (pH 6.8), HCl buffer (pH 1.2), and distilled water, was used in a volume of 500 mL. By incorporating drug loaded nanometrices in dialysis membranes with molecular cutoffs between 12 and 14 kDa and sealing the ends, *in-vitro* dissolution tests were carried out. Dialysis membranes laden with drug loaded nanometrices were then fastened with peddles. The temperature was kept at 37°C ± 2°C throughout, and the pedals were submerged in baskets containing the appropriate media and allowed to rotate at 50 rpm. To ensure the consistency of the dissolving media volume, 5 mL samples were periodically collected from the basket and afterwards substituted with an equal volume of dissolution media. The examination of obtained materials was conducted using a UV-Visible spectrophotometer (UV 3000, Germany). By using a UV spectrophotometer set at λ_{\max} 254 nm, the amount of the drug that was released in the respective medium was determined. To obtain the accepted statistical value, the data were examined three times.

2.3.11 Solubility studies

The comparative solubility studies of the fabricated nanometrices and raw counterpart (pure ACV) were carried out to access the impact on solubility enhancement of the ACV in nanometrices. The solubility studies were performed in aqueous medium and buffer solutions of respective pH 1.2 and 6.8. A significant quantity of ACV was incorporated into the distilled water and also in each of the two buffer solutions. The suspensions were kept on shaking through a mechanical shaker at a temperature of 25°C for 24 h. Similar procedure was adopted for the formulated nanometrices but in this process, however; the nanometrices equivalent to 25 mg of ACV was added to the distilled water and into the two buffer solutions as well. After 24 h, the suspensions were placed in a static position for 2 h without stirring followed by centrifugation with 20,000 rpm for 10 min. After centrifugation, the suspension was filtered and the filtrate was then analyzed spectroscopically through UV instrument at λ_{\max} 254 nm.

2.3.12 Stability evaluations

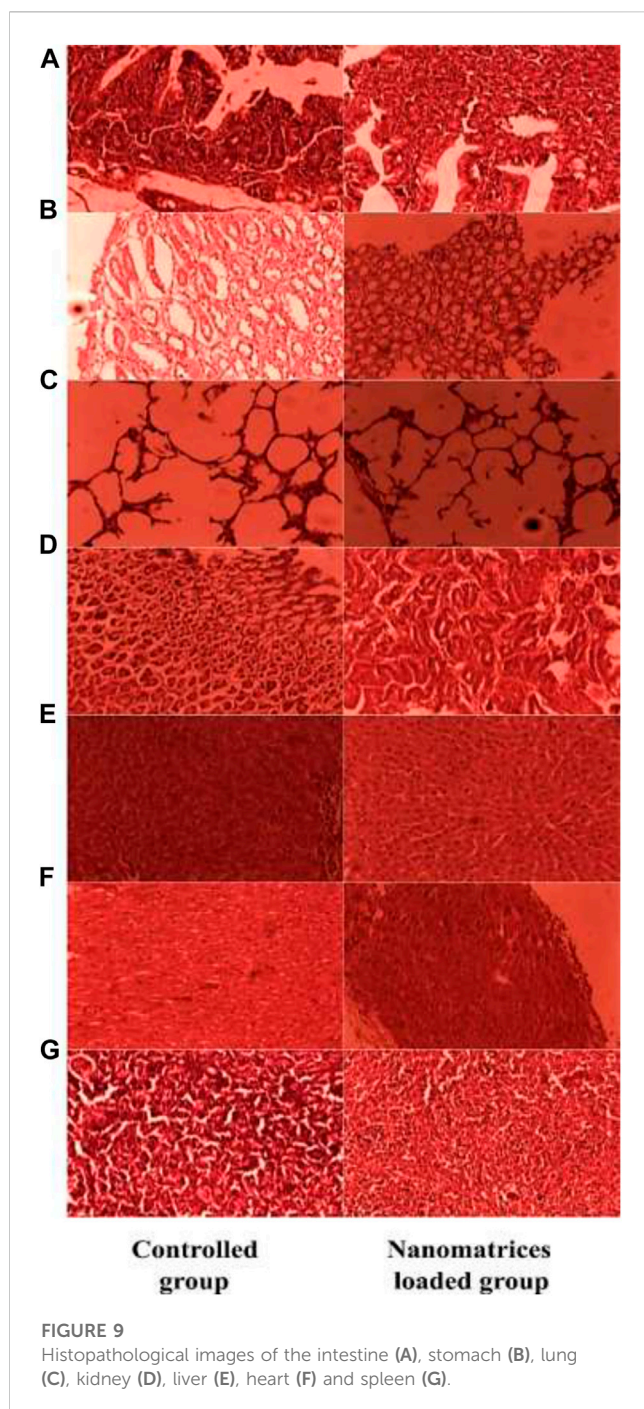
The stability experiments of nanometrices loaded with ACV were conducted in accordance with established ICH principles and a previously outlined methodology (Badshah et al., 2023a). Formulated nanometrices were stored in a stability chamber at 40°C ± 2°C with 75% ± 5% RH in airtight glass vials with sealing systems. The sampling was planned for the months of 0 months, 3 months, and 6 months. The effectiveness of solubilization, drug loading (%), FTIR spectra, and physical appearance changes were all evaluated.

2.3.13 Statistical analysis

The statistical analysis of swelling experiments and percent drug release was conducted using IBM® SPSS® statistics version 24 software, with a significance threshold of 5%. The verification of results for swelling and *in-vitro* drug release was conducted using statistical methods including paired sample t-test, univariate analysis, and *post hoc* multiple comparison.

3 Toxicological evaluations

Toxicological studies were carried out as per standard Laboratory animals guidelines of National Institutes of Health (NIH) (NIH Publications No. 8023, revised 1978) (Chen et al., 2019). In addition, the protocols as approved by the institutional



research ethics committee (IREC) were followed in handling and care of animals under reference number IREC-17-2021. Six healthy rabbits were habituated for 2 weeks in clean enclosures. Two groups each consisting of three rabbits were established. Rabbits of group I were marked as control and were provided with water and food. Along with access to water and food, group II rabbits were orally administered with 5 g/kg body weight of nanometrices. Physical observations of the rabbits, mortality rate, rabbits' weight, diet, and intake of water by rabbits were precisely observed. After habituating for 2 weeks under thorough observations, rabbits of both groups were processed for collection of blood samples and vital organs in order to examine the biochemistry of blood and histopathology.

4 Results and discussion

4.1 Visual examination

The uniform structure was shown by fabricated nanometrices (Figure 1). During the formulation process, a whitish gel-like mass was obtained. The surface of the nanometrices was porous to partial porous with significant gelling characteristics. The formulated nanometrices were initially white which showed slight shedding upon swelling. They were fluffy in appearance and showed good flow behavior.

4.2 Particle size

Nano-scale drug delivery systems offer numerous advantages compared to conventional macro-scale dosage forms. Due to their nanoscale dimensions, nanoparticles possess a significant surface area, which facilitates the encapsulation of drugs with low water solubility within their cavities and promotes efficient absorption of dissolving medium. The aforementioned attributes have the potential to augment the solubility and hence the bioavailability of drugs that exhibit low water solubility (Ahmad et al., 2023). The reduction in the size of the particles generally leads to a large surface area which ultimately enhances the dissolution rate (Alam et al., 2022). The average hydrodynamic diameter of the optimized nanometrices was 237.53 ± 7.32 nm. The polydispersity index was found to be 0.410. The small value of the polydispersity index of the polydisperse nanometrices revealed that formulation has a low tendency to form clusters. Moreover, the zeta potential value was found to be -32.91 ± 5.72 mV. A stable system usually has a zeta potential value of more than 30 mV. Higher zeta potential values, whether positive or negative, typically result in stronger repulsion forces, little aggregate formation, and simple redispersion of the particles. Similarly, the particle size of the drug-loaded nanometrices was 25 nm higher than that of the unloaded nanometrices. The increase in the particle size of the drug loaded nanometrices may be linked with the fact that as poorly soluble hydrophobic agent was loaded inside the system, it showed a repulsive behavior with that of the hydrophobic core of the nanometrices. Particle size was increased as a result of the repellent process between the hydrophobic drug and the hydrophobic core. Table 2 lists the corresponding particle sizes of all the nanometrices, both loaded and unloaded, together with their polydispersity indices and zeta potential values.

4.3 Scanning electron microscopy

The loading and distribution of drugs are contingent upon the surface morphology of the delivery system, which plays a crucial role in this process. Visual representations of the fabricated nanometrices were recorded at different resolutions. As seen in Figure 2, the images obtained showed that the formulated nanometrices have a fluffy and porous structure. The system's porosity aids in the effusion and diffusion of the drug and dissolving media. To increase the solubility of

chlorthalidone, Badshah et al. formulated nanometrices and reported similar characteristics (Badshah et al., 2021). Enhancement in the solubility of poorly soluble drugs is highly dependent on the high porosity of the system (Borba et al., 2016). Being having porous morphology, a significant quantity of drug as revealed in Table 2, was encapsulated inside the fabricated system.

4.4 Powder X-Ray diffraction (PXRD)

The amorphous or crystalline form of the moiety plays a significant role in solubility. As per the literature review, it has been found that amorphous form of any moiety has significant solubility as compared to the crystalline form. PCL is a crystalline polymer and the powder X-Ray diffractogram of pure PCL has shown two characteristic peaks at 2θ of 21.2° and 23.6° (Figure 3A). PXRD of PEG-6000 showed two intense peaks at 2θ of 19.41° and 23.34° (Figure 3B). Comparable peaks of PEG-6000 were reported in an already reported study (Etman et al., 2017). Some minor peaks were also observed at $2\theta = 26.30^\circ, 35.18^\circ, 38.63^\circ$ and 46.12° which were in comparison with the previously reported study (Jayaramudu et al., 2016). β -CD showed characteristic peaks (Figure 3C) at 2θ of $5.75^\circ, 7.90^\circ, 22.23^\circ, 23.03^\circ, 24.85^\circ$ and 28° (Badshah et al., 2021). PXRD of ACV showed observable peaks at $2\theta = 23.68^\circ, 25.64^\circ, 26.16^\circ$ and 29.08° which demonstrated and confirmed the crystalline nature of the drug (Figure 3D). Similar peaks were also reported in a study where controlled delivery of ACV was achieved by loading it in developed hydrogels (Al-Tabakha et al., 2021). When PXRD pattern of the drug loaded nanometrices was studied, it was found that the intense peaks of polymers and crystalline drug were suppressed as shown in Figure 3E. This suppression of the intense peaks of the polymers and that of the drug confirms that an amorphous system has been formulated. The resultant amorphous system has substantial role in the aqueous solubility of the poorly soluble drug (Mahmood et al., 2016b).

4.5 FTIR spectroscopy

Spectroscopy is a noteworthy scientific process that can be applied to both crystalline and amorphous materials. The evaluation of a crosslinked network, compatibility, and drug entrapment inside the polymeric network was conducted by the utilization of FTIR spectroscopy on both the individual components, unloaded and loaded nanometrices. Spectroscopy was performed in $4,000\text{--}600\text{ cm}^{-1}$ wavelength range. The obtained spectrograms were compared and results were noted. FTIR spectroscopy showed significant and observable peaks at different wave numbers. The drug showed an observable peak at $3,442\text{ cm}^{-1}$, which was due to --OH stretching vibrations (Figure 4A). The peaks at $3,238\text{ cm}^{-1}, 2,930\text{ cm}^{-1}, 1,741\text{ cm}^{-1}, 1,479\text{ cm}^{-1}$ and $1,182\text{ cm}^{-1}$ were due to the stretching vibration peaks of --NH , aliphatic --CH , --C=O , --C=N and --C--O--C-- functional groups (Jana et al., 2016). Spectrogram of PCL obtained showed various peaks at different wave numbers which were subjected to various functional groups. The peaks of PCL obtained showed C--O--C at $1,236\text{ cm}^{-1}$, the peak was due to --C--O--C-- at $1,171\text{ cm}^{-1}, 1,722\text{ cm}^{-1}$ was related to CH_2 whereas the

peak at $3,443\text{ cm}^{-1}$ was associated to the functional group OH (Figure 4B). Similar peaks of the PCL were reported in a prior work that was intended to electrospun scaffolds made of a polycaprolactone/polyurethane composite with graphene oxide for skin tissue engineering (Sadeghianmaryan et al., 2020a). When the spectrogram of the PEG-6000 was studied (Figure 4C), different peaks were observed which were due to the existence of the various functional groups. PEG-6000 spectrum showed a peak at $2,887\text{ cm}^{-1}$ and it was related to the stretching vibrations of C--H . Bending vibrations due to C--H were observed at wave number $1,464\text{ cm}^{-1}$. O--H stretching vibrations showed a peak at $1,297\text{ cm}^{-1}$. Moreover, the peaks at $1,109\text{ cm}^{-1}$ and $1,094\text{ cm}^{-1}$ were related to C--O--H and C--O--H groups respectively. Khan et al. reported peaks of PEG-6000 which were in similar wave number as mentioned above (Khan R. et al., 2022). A broad transmittance peak at wave number $3,300.92\text{ cm}^{-1}$ in the spectrum of β -CD was because of --OH stretching vibration (Figure 4D). Similarly, at wave number $2,920.52\text{ cm}^{-1}$, due to --CH , stretching vibrations were observed whereas at $1,643.60\text{ cm}^{-1}$, due to C--O , the asymmetric stretching vibrations were recorded. A specific band because of coupling vibrations of C--O and C--C was recorded at $1,024.01\text{ cm}^{-1}$. All the demonstrated bands and wave numbers were in resemblance to the previously reported research work (Malik et al., 2017). The FTIR spectrum of MAA as shown in (Figure 4E) depicted a specific peak at $2,929\text{ cm}^{-1}$ which was due to the presence of methyl C--H asymmetric stretching. The peaks ranging from $1,725\text{ cm}^{-1}$ to $1,700\text{ cm}^{-1}$ indicated the presence of carboxylic acid groups. The C=C stretching vibrations were related to the peak number $1,633\text{ cm}^{-1}$ (Barkat et al., 2017). When the unloaded nanometrices spectrum was observed (Figure 4F), it was found that the majority of the peaks of the individual components were present at the same wave number. There was slight shifting of the peaks either to higher or lower level but no significant shift was noted. Similarly, during the study of the spectrum of the unloaded nanometrices, some new characteristic peaks were also observed which indicated the formation of some new bonds during polymerization reaction. Since, the corresponding peaks were present in their specific position, some slight shifting was also observed and also some new peaks were noted in the spectrum of unloaded nanometrices, it can be stated that successful crosslinking of the components has been achieved and a crosslinked polymeric system has been formulated. The characteristic peaks of the drug were also present in their original positions when the spectrum of the drug loaded nanometrices (Figure 4G) was examined, indicating that there had been no chemical interactions between the drug and the other components and that the drug entities had been significantly loaded inside the structure without undergoing any changes in its chemical structure.

4.6 Thermogravimetric analysis (TGA)

Pure drug ACV (Figure 5A) showed a thermal activity near the temperature range of 263.57°C , which may be attributed to the melting point of the drug. Similarly, an additional narrow dip was observed at a temperature near 100°C , which was linked with 1.5% of the total weight loss. It might be due to the evaporation of the water in the form of vapors (Nagra et al., 2022). Moreover, the significant

weight loss of 25% in the range of 250°C–300°C may be due to the destruction of the ACV (Akbari et al., 2020). Pure PEG-6000 (Figure 5B) started initial decomposition at a temperature range of 350°C (Wu et al., 2017). Abrupt melting of PEG-6000 was observed at a temperature range of 400°C. While the complete loss of the weight of the PEG-6000 of 100% was around 440°C. Comparable values of the TGA analysis of the PEG-6000 were also reported in a previous study (Zahir et al., 2019). Thermal decomposition of PCL was initiated after the temperature range of 250 °C (Bagheri and Mahmoodzadeh, 2020). TGA of PCL as shown in Figure 5C depicted a weight loss due to the thermal degradation which started at around the temperature range of 325.5°C, with approximately an initial weight loss of 23% at a temperature of 397.7 °C. Similar thermal degradation of PCL was reported in a previously reported study (Sadeghianmaryan et al., 2020b). When the TGA thermogram of β -CD was studied (Figure 5D), it was observed that a gradual reduction in the mass of the β -CD occurred. At a temperature range of 359 °C, a total of 84.28% mass was lost and only 15.72% mass was left (Badshah et al., 2023b). When TGA thermogram of nanometrices loaded with the drug was studied as presented in Figure 5E, it was found that reduction in the mass of the formulated nanometrices was reduced at the specified temperature ranges of the individual components. Additional peaks were seen and documented in the TGA thermogram of the nanometrices, suggesting the development of a novel polymeric network characterized by improved thermal stability. In a prior investigation, comparable attributes were identified, leading to the assertion that these attributes substantiate the development of a novel formulation that exhibits thermal stability (Sarfriz et al., 2017).

4.7 Sol-gel fraction

A fraction analysis utilizing sol-gel was performed in order to determine the magnitude of unreacted components. Table 3 illustrates the relationship between polymers and monomer concentrations and the gel and sol fractions. It is observed that as the concentrations of polymers and monomer increase, the gel fraction exhibits a progressive growth, while the sol fraction experiences a fall. The observed correlation between higher polymers and monomer concentrations and an increased gel fraction can be attributed to the availability of a greater number of active sites for the polymerization reaction as the concentration is raised. The augmentation of active sites enhanced the process of polymerization, leading to the formation of a stable network. Furthermore, the polymerization process took place during its first phase, leading to the complete consumption of the additional materials. Additionally, a drop in the gel fraction and a rise in the sol fraction were seen as the concentration of the crosslinker MBA was raised. Although the majority of researchers claim that when MBA concentration is increased, the gel fraction is increased as well (Fekete et al., 2016), however, in our analysis, we discovered that the gel fraction fell as crosslinker concentration rose. The lack of sufficient free radicals (active sites) of polymers and monomer for the polymerization reaction may be the cause of the lower gel fraction with increased MBA concentration. As a result, there was a drop in the gel fraction and an increase in the sol fraction. An earlier study also reported the similar findings that were consistent with ours (Khan et al., 2021).

4.8 Swelling study

Swelling plays a critical role in the drug mobility and release from the carrier system (Abou Taleb et al., 2015). It is directly connected to how the drug is released (Bode et al., 2019). Significant swelling causes the drug to be released from the polymeric system effectively. As illustrated in Figure 6, the swelling study was carried out at pH 1.2 and 6.8. At pH 6.8, all formulations exhibited more swelling than they did at pH 1.2. The MAA carboxylate ion content is responsible for this phenomenon. Since 5.65 is the pKa of MAA (Bukhari et al., 2015), consequently, there will be an increase in the ionization of the MAA as the pH of the swelling media rises from the value of pKa. The carboxylate groups (COOH to COO⁻) will become ionized at a pH greater than the pKa of MAA. An increase in the COO⁻ will enhance the intensity of repulsion at higher pH and thus extensive and significant swelling will be obtained (Rafique et al., 2022). The study focused on investigating the influence of variable concentrations of polymers, monomer, and cross linker, as well as different pH levels, on the swelling behavior of nanometrices. The effects of elevated concentrations of polymers, monomer, and cross-linker on system swelling were observed. Within a span of 10 min, a sudden increase in swelling occurred, which can be attributed to the hydrophilic properties, significant surface area, and nanoscale dimensions of the nanometrices. The system swelled more when the concentrations of PEG, PCL, and β -CD were enhanced. Increased number of functional units for monomer to be grafted may be the cause of the swelling that increases with increasing polymers' concentrations. Moreover, PEG and β -CD are hydrophilic polymers and increasing the concentrations of PEG and β -CD resulted in the availability of large number of hydrophilic units, which ultimately supported the enhanced swelling of the nanometrices with increased concentrations of the polymers. Increased swelling was observed in the formulations NMT-1 and MNT-2. Further increase in the concentration of the polymers in formulation NMT-3, resulted in decreased swelling. This decreased swelling may be linked with the formation of dense network. Increased concentrations of the polymers resulted in a dense network. Although functional units for grafting were increased but since a dense system was also generated, therefore, it was difficult for the swelling media to penetrate in sufficient amount inside the system, and hence decreased swelling was noted. Similar to how the monomer concentration rose, a significant swelling was obtained. This is explained by the presence of the carboxylate group in MAA's chemical structure. The concentration of the carboxylate groups also grew along with the MAA concentration, which upon ionization produced an intense electrostatic repulsion between the ionized COO⁻ groups. Due to the intense electrostatic repulsion between the carboxylate groups when they are ionized, swelling increased as MAA concentration was evaluated. An earlier study with similar results found that swelling behavior increased with a rise in MAA concentration (Batool et al., 2022). The concentration of the crosslinker is a significant factor that influences the swelling capacity of the nanometrices. Different concentrations of the crosslinker were employed, and the impact on swelling was observed. The decrease in system swelling was observed with an increase in the concentration of the crosslinker. The observed results indicated a restricted degree of swelling at both pH 1.2 and pH 6.8.

By increasing the concentration of the crosslinker, a network with a high degree of crosslinking and density was generated. The diffusion of the swelling medium into the system was limited by the density and extent of crosslinking within the network. The expansion capacity of the system was reduced due to inadequate influx of the medium into the system. A previous study yielded a comparable result, demonstrating a negative correlation between an increase in MBA concentration and system's swelling (Siddiqua et al., 2022).

4.9 Percent drug loading

Since drug was loaded into the formulated nanometrices by post-formation loading method, therefore, the drug was encapsulated in the formulated system after the formulation process was completed. More than 70% drug loading was observed in all the formulations with the most protuberant loading in the formulation NMT-6, where more than 80% of the loading was noted as shown in Table 3. NMT-6 showed significant and prominent swelling among all the nanometrices, which supported maximized loading of the drug. Similarly, minimum drug loading among all the formulations was shown by NMT-8 and NMT-9. This reduced drug loading in both formulations may be related to the crosslinker's concentration being increased. The growing crosslinker concentration produced a highly crosslinked and dense network. This highly crosslinked and dense network made it challenging for the solvent to diffuse through it, which impeded the considerable flow of drug-loaded medium across the system. Additionally, the strongly crosslinked dense network hampered the swelling of both formulations. In the loading and release of drug, swelling is crucial (Kabanov and Vinogradov, 2009). The combination of the aforementioned characteristics prevented the drug from loading significantly into the system's core, which is why only minimal drug loading was seen in both formulations.

4.10 *In vitro* release study

In-vitro release behavior of the drug from the fabricated nanometrices was performed in pH 1.2, 6.8, and in water to access the response of the system to various dissolution media. From the obtained data, it was noted that formulated nanometrices showed enhanced and significant drug release in aqueous media and in buffer 6.8 as compared to that of pH 1.2 (Figures 7A, B). Although, the polymeric nanometrices showed different responses in various dissolution media but over all a satisfactory drug release profile was obtained. In every dissolution medium used for the release of the drug, all formulations had a drug release rate of greater than 70%. The ionization of the carboxylic acid groups contained in the monomer MAA is what causes the highest drug release in an aqueous medium and at pH 6.8 as opposed to that of pH 1.2. The COOH groups present in the monomer of MAA will become ionized at pH values higher than the pKa value of MAA, which will result in the ionization of the carboxylic acid group and the production of the COO⁻ functional group, as was already explained in the swelling section. Significant swelling will be seen as a result of the considerable electrostatic repulsion caused by the

rise in the concentration of COO⁻ functional groups in the polymeric system. The release of the drug will be at its highest in pH 6.8 and water compared to pH 1.2 because swelling of the system directly affects drug release. At pH 1.2, there is little to no ionization of the functional groups, which prevents the system from expanding extensively and significantly, limiting the amount of drug released significantly. In a basic media, the polymeric chains expand, causing increased swelling and considerable release of drug (Özkahraman et al., 2022). With the increase in concentration of the polymers, there was an increase in the release pattern of the drug in formulations NMT-1 to NMT-2. Further increase in polymeric contents in formulation NMT-3, the release pattern was reduced as compared to that of previous formulations, i.e., NMT-1 and NMT-2. The systemic swelling behavior may be related to the increase in drug release that occurs as polymeric concentrations rise. Most of the drug that was entrapped in the polymeric nanometrices was released from the system as the swelling of the system increased along with the polymers' concentration. This is because of the swelling behavior, as explained, is directly related to the release of the drug. The release of the drug was decreased in the formulation NMT-3, having continued increase in polymeric contents. The result was a dense network that was substantially crosslinked. Because of the restricted diffusion of the dissolving media inside the system, the system was unable to inflate much, which lowered the amount of drug release. There was an increase in the drug's release when the MAA's concentration was raised. As the monomer concentration rose, a significant amount of drug was released (Shabir et al., 2017). Significant release of the formulations with increased concentration of the MAA can be linked with the presence of the carboxylate groups. Ionization of the carboxylate groups in to the COO⁻ ions resulted in electrostatic repulsion among the anions. The electrostatic repulsion will be significant when higher contents of the monomer will be used. This repulsion will result in extensive swelling behavior and hence significant swelling of the system will be obtained which will ultimately increase the release of the drug and a significant amount of the drug will be released. In a previous study conducted for the formulation of pH-sensitive hydrogels for release of Nadolol, a similar result was obtained where increased monomeric contents resulted in increased drug release and *vice versa* (Bal et al., 2016). The release of the drug was reduced as a result of the crosslinker MBA's concentration being increased. A dense network with a substantially crosslinked structure was produced by the enhanced crosslinker concentrations. The system was unable to inflate appreciably, which prevented the dissolving medium from flowing freely inside the system. As a result, there was little diffusion of the loaded drug out of the system, and no noticeable drug release behavior was noticed. Similar results were also noted in a prior investigation, where it was discovered that a higher concentration of the crosslinker MBA decreased drug release (Barkat et al., 2017; Barkat et al., 2018). Additionally, the drug release patterns of the formulations were contrasted with those of a commercially available brand of acyclovir (Acylex[®]) in pH values of 1.2, 6.8, and aqueous medium. Comparing the release of the drug from the formulations and that of the marketed brand, a notable difference was seen. While the marketed brand only demonstrated a limited release of the drug within the same time frame, formulations were able to release the maximal amount of the drug in a short

length of time. Figures 6A,B shows the drug release from the formulations and that of the marketed tablet at various dissolution mediums.

4.11 Solubility studies

Amphoteric moiety acyclovir exhibits solubility at pH 1.2 as well as at pH levels over 7.4. At pHs of 1.2, 6.8, and aqueous medium, pure ACV showed solubility profiles of 2.10 mg/mL, 1.55 mg/mL, and 1.2 mg/mL, respectively (Figure 8). When the fabricated nanometrices' solubility profiles were compared to those of the drug alone in various mediums, it was found that the nanometrices had improved solubility profiles. The NMT-6 formulation showed improved solubility as compared to other formulations and it was based on the results of swelling and *in-vitro* drug release. NMT-6 showed notable swelling and drug release results. As compared to the drug alone, the aforementioned formulation significantly improved the solubility profile of ACV. In pH 1.2, the drug's solubility increased by 12.66 folds, pH 6.8 by 9.07 folds, and 10.69 folds in water by the optimized formulation NMT-6. The fact that the fabricated nanometrices were able to improve the solubility profile of ACV may be related to the nanometrices' ability to do so due to their reduced size, increased surface area, and amorphousness. Additionally, the polymers PCL, PEG-6000 and β -CD were used, which helped to improve the drug's solubility. Three polymers and a monomer were combined to create a complex that was well-suited to encapsulate the hydrophobic drug inside of, concealing the hydrophobic properties and improving the solubility of the drug.

4.12 Stability evaluations

To ascertain the stability of the synthesized nanometrices during the given period, stability experiments were carried out. Different parameters like physical appearance, FTIR spectra, percent drug loading and swelling ability were monitored and it was found that no significant change occurred in any of the above-mentioned parameters. The results obtained from the performed studies have been mentioned in Table 4.

4.13 Statistical analysis

The Post Hoc test was employed to conduct multiple comparisons of the dynamic swelling of nanometrices at pH 6.8 and 1.2. The results of the Post Hoc test, as determined through Univariate analysis, indicated that there was no significant difference in the dynamic swelling of all formulations at pH 6.8. This was evidenced by the *p*-values being greater than 0.05 for all formulations. However, it was observed that NMT-8 and NMT-9 nanometrices exhibited a significant difference from NMT-7. This difference can be attributed to the higher concentration of cross-linker present in NMT-8 and NMT-9 compared to the other formulations. Likewise, at pH 1.2, significant differences were observed between NMT-9 and NMT-1, NMT-8 and NMT-2, NMT-8 and NMT-9, NMT-3, NMT-9 and NMT-4, NMT-8 and

NMT-9, NMT-5 and NMT-6, as well as NMT-9 and NMT-7. The increased amount of cross-linker in NMT-8 and NMT-9, relative to the other formulations, is the underlying reason for these significant differences. This is supported by the *p*-values being less than 0.05, indicating statistical significance. A paired sample t-test was used to compare the *in-vitro* drug release experiments at pH 6.8 and pH 1.2 for all formulations. The results obtained from the comparison of *in-vitro* drug releases of all nanometrices indicated a lack of significant difference, as evidenced by a *p*-value exceeding 0.05 or 5%. However, formulation NMT-9 exhibited a statistically significant difference, as indicated by a *p*-value of less than 0.05 or 5%. The NMT-9 sample has the most elevated concentration of cross-linker. The Post Hoc test was conducted to do numerous comparisons of the *in-vitro* drug release study of nanometrices at pH 6.8 and pH 1.2. All formulations exhibited no significant difference at a pH of 6.8, as shown by a *p*-value greater than 5% or 0.05. For a pH of 1.2, all formulations exhibited no significant difference, as shown by a *p*-value greater than 5% or 0.05. Nevertheless, there was a notable distinction between NMT-9 and both NMT-5 and NMT-6. NMT-9 exhibited the highest concentration of cross-linker, but NMT-5 and NMT-6 demonstrate an ascending sequence of monomer content. The larger concentration of cross-linker limited the swelling of NMT-9, resulting in maximum swelling and enhanced drug release for NMT-5 and NMT-6.

5 Toxicological evaluations

A toxicological investigation was conducted to determine the safety profile and biocompatibility of the synthesised nanometrices with the vital organs. During the investigation, several characteristics related to the safety profile were assessed. None of the parameters showed any observable difference. The rabbits of both groups neither showed any sign of illness, tremors, stomach disturbance nor any dermal and ocular irritation was found. Similarly, no alteration was found in the intake of food, water, and behavior of the animals during and after the study. After the study, the weight of the vital organs was also performed and no prominent change was observed between the control and treated group. Similarly, all the biochemical parameters of the blood and that of the vital organs of both the control and tested group were in comparison and no significant difference was observed. All the above findings confirmed the safety of the formulated nanometrices and they were found to be biocompatible with the vital organs. In a study performed earlier, a similar toxicological investigation was performed and the synthesized system was found to be biocompatible with the biological system (Barkat et al., 2018). Tables 5–8 present the findings regarding the clinical observations from the acute oral toxicity test, the effects of optimized blank nanometrices (NMT-6) on weight variation (g) of various organs during histopathological observation, the biochemical analysis of blood of animals treated with blank nanometrices, and the biochemical analysis of the liver, kidneys, and lipid profiles of rabbits in the control and nanometrices treated group. Similarly, the histopathological images of the vital organs from both the controlled and tested group can also be seen in Figure 9. No significant difference or change was observed.

6 Conclusion

An extremely swellable and stable drug delivery system was designed and formulated which significantly enhanced the solubility of the poorly aqueous soluble drug. The system was biocompatible with the vital organs and that of the other systems of the tested animals. All the structural characterization of the formulated nanometrices confirmed that the formulated system is quite suitable to enhance the solubility of the poorly aqueous soluble drug. Moreover, being highly swellable, the system was able to release maximum amount of the drug in the dissolution medium. The *in-vitro* characteristics of the system were also satisfactory. The aforementioned statements led to the conclusion that the developed nanometrices can be employed to improve the solubility of other drugs with low water solubility, regardless of toxicological or biocompatible concerns.

Data availability statement

The raw data supporting the conclusion of this article will be made available by the authors, without undue reservation.

Ethics statement

The animal study was approved by The current research is approved by the ethical review committee of the University of Lahore, Lahore, Pakistan under reference number IREC-17-2021. Notably, all animal experimentation was conducted in accordance with applicable laws, regulations, and guidelines, prioritizing animal welfare and minimizing any potential harm. The study was conducted in accordance with the local legislation and institutional requirements.

Author contributions

AU: Investigation, Writing–original draft. KB: Visualization, Writing–original draft. SH: Conceptualization, Writing–original draft. MA: Data curation, Writing–original draft. SB: Validation, Writing–original draft. AA: Software, Writing–review and editing. IA:

Resources, Writing–review and editing. YB: Software, Writing–original draft. H-AN: Formal Analysis, Writing–review and editing. MD: Writing–original draft. MB: Methodology, Writing–review and editing.

Funding

The author(s) declare financial support was received for the research, authorship, and/or publication of this article. This work is financially supported by the Researchers Supporting Project (RSP2023R457). King Saud University, Riyadh, Saudi Arabia.

Acknowledgments

All authors are thankful to Higher Education Commission (HEC) of Pakistan, for providing and funding of NRPU project number 7233 to compete this research project. The authors are also thankful to The Faculty of Pharmacy, The University of Lahore, Pakistan for providing lab facilities and other equipment to accomplish this project. The authors also would like to extend their sincere appreciation to the Researchers Supporting Project, King Saud University, Riyadh, Saudi Arabia for funding this work through the project number (RSP2023R457).

Conflict of interest

The authors declare that the research was conducted in the absence of any commercial or financial relationships that could be construed as a potential conflict of interest.

Publisher's note

All claims expressed in this article are solely those of the authors and do not necessarily represent those of their affiliated organizations, or those of the publisher, the editors and the reviewers. Any product that may be evaluated in this article, or claim that may be made by its manufacturer, is not guaranteed or endorsed by the publisher.

References

- Abou Taleb, M. F., Alkahtani, A., and Mohamed, S. K. (2015). Radiation synthesis and characterization of sodium alginate/chitosan/hydroxyapatite nanocomposite hydrogels: a drug delivery system for liver cancer. *Polym. Bull.* 72, 725–742. doi:10.1007/s00289-015-1301-z
- Ahmad, M. A., Javed, R., Adeel, M., Rizwan, M., and Yang, Y. (2020). PEG 6000-stimulated drought stress improves the attributes of *in vitro* growth, steviol glycosides production, and antioxidant activities in *Stevia rebaudiana bertonii*. *Plants* 9 (11), 1552. doi:10.3390/plants9111552
- Ahmad, W., Khalid, I., Barkat, K., Minhas, M. U., Khan, I. U., Syed, H. K., et al. (2023). Development and evaluation of polymeric nanogels to enhance solubility of letrozole. *Polym. Bull.* 80 (4), 4085–4116. doi:10.1007/s00289-022-04248-5
- Akbari, M., Ghasemzadeh, M. A., and Fadaeian, M. (2020). Synthesis and application of ZIF-8 MOF incorporated in a TiO₂@Chitosan nanocomposite as a strong nanocarrier for the drug delivery of acyclovir. *ChemistrySelect* 5 (46), 14564–14571. doi:10.1002/slct.202003213
- Alam, A., Jawaid, T., Alsanad, S. M., Kamal, M., Rawat, P., Singh, V., et al. (2022). Solubility enhancement, formulation development, and antibacterial activity of xanthan-gum-stabilized colloidal gold nanogel of hesperidin against *Proteus vulgaris*. *Gels* 8 (10), 655. doi:10.3390/gels8100655
- Al-Tabakha, M. M., Khan, S. A., Ashames, A., Ullah, H., Ullah, K., Murtaza, G., et al. (2021). Synthesis, characterization and safety evaluation of sericin-based hydrogels for controlled delivery of acyclovir. *Pharmaceuticals* 14 (3), 234. doi:10.3390/ph14030234
- Altun, E., Ahmed, J., Onur Aydogdu, M., Harker, A., and Edirisinghe, M. (2022). The effect of solvent and pressure on polycaprolactone solutions for particle and fibre formation. *Eur. Polym. J.* 173, 111300. doi:10.1016/j.eurpolymj.2022.111300
- Asghar, S., Akhtar, N., Minhas, M. U., and Khan, K. U. (2021). Bi-polymeric spongy matrices through cross-linking polymerization: synthesized and evaluated for solubility enhancement of acyclovir. *AAPS PharmSciTech* 22 (5), 181. doi:10.1208/s12249-021-02054-2

- Badshah, S. F., Akhtar, N., Minhas, M. U., Khan, K. U., Khan, S., Abdullah, O., et al. (2021). Porous and highly responsive cross-linked β -cyclodextrin based nanomatrices for improvement in drug dissolution and absorption. *Life Sci.* 267, 118931. doi:10.1016/j.lfs.2020.118931
- Badshah, D., Minhas, M. U., Khan, K. U., Barkat, K., Abdullah, O., Munir, A., et al. (2023a). Structural and *in-vitro* characterization of highly swellable B-cyclodextrin polymeric nanogels fabricated by free radical polymerization for solubility enhancement of Rosuvastatin. JDDST-D-22-01017.
- Badshah, S. F., Minhas, M. U., Khan, K. U., Barkat, K., Abdullah, O., Munir, A., et al. (2023b). Structural and *in-vitro* characterization of highly swellable β -cyclodextrin polymeric nanogels fabricated by free radical polymerization for solubility enhancement of rosuvastatin. *Part. Sci. Technol.*, 1–15. doi:10.1080/02726351.2023.2183161
- Bagheri, M., and Mahmoodzadeh, A. (2020). Polycaprolactone/graphene nanocomposites: synthesis, characterization and mechanical properties of electrospun nanofibers. *J. Inorg. Organomet. Polym. Mater.* 30 (5), 1566–1577. doi:10.1007/s10904-019-01340-8
- Bal, A., Özkahraman, B., and Özbaşı, Z. (2016). Preparation and characterization of pH responsive poly(methacrylic acid-acrylamide-N-hydroxyethyl acrylamide) hydrogels for drug delivery systems. *J. Appl. Polym. Sci.* 133 (13). doi:10.1002/app.43226
- Barkat, K., Ahmad, M., Minhas, M. U., and Khalid, I. (2017). Oxaliplatin-loaded crosslinked polymeric network of chondroitin sulfate-co-poly(methacrylic acid) for colorectal cancer: its toxicological evaluation. *J. Appl. Polym. Sci.* 134 (38), 45312. doi:10.1002/app.45312
- Barkat, K., Ahmad, M., Usman Minhas, M., Khalid, I., and Nasir, B. (2018). Development and characterization of pH-responsive polyethylene glycol-co-poly(methacrylic acid) polymeric network system for colon target delivery of oxaliplatin: its acute oral toxicity study. *Adv. Polym. Technol.* 37 (6), 1806–1822. doi:10.1002/adv.21840
- Batool, N., Sarfraz, R. M., Mahmood, A., Zaman, M., Zafar, N., Salawi, A., et al. (2022). Orally administered, biodegradable and biocompatible hydroxypropyl- β -cyclodextrin grafted poly(methacrylic acid) hydrogel for pH sensitive sustained anticancer drug delivery. *Gels* 8 (3), 190. doi:10.3390/gels8030190
- Bode, C., Kranz, H., Fievez, A., Siepmann, F., and Siepmann, J. (2019). Often neglected: PLGA/PLA swelling orchestrates drug release: HME implants. *J. Control. Release* 306, 97–107. doi:10.1016/j.jconrel.2019.05.039
- Borba, P. A. A., Pinotti, M., de Campos, C. E. M., Pezzini, B. R., and Stulzer, H. K. (2016). Sodium alginate as a potential carrier in solid dispersion formulations to enhance dissolution rate and apparent water solubility of BCS II drugs. *Carbohydr. Polym.* 137, 350–359. doi:10.1016/j.carbpol.2015.10.070
- Bukhari, S. M. H., Khan, S., Rehanullah, M., and Ranjha, N. M. (2015). Synthesis and characterization of chemically cross-linked acrylic acid/gelatin hydrogels: effect of pH and composition on swelling and drug release. *Int. J. Polym. Sci.* 2015, 1–15. doi:10.1155/2015/187961
- Chen, J., Liu, J., Zhou, B., Song, Q., Sun, W., and Yuan, Y. (2019). Toxicity studies for the use of prodrug of voriconazole in rats. *Regul. Toxicol. Pharmacol.* 104, 8–13. doi:10.1016/j.yrtph.2019.02.013
- Chivere, V. T., Kondiah, P. P. D., Choonara, Y. E., and Pillay, V. (2020). Nanotechnology-based biopolymeric oral delivery platforms for advanced cancer treatment. *Cancers* 12 (2), 522. doi:10.3390/cancers12020522
- Dong, B., and Hadinoto, K. (2019). Carboxymethyl cellulose is a superior polyanion to dextran sulfate in stabilizing and enhancing the solubility of amorphous drug-polyelectrolyte nanoparticle complex. *Int. J. Biol. Macromol.* 139, 500–508. doi:10.1016/j.jbiomac.2019.08.023
- Etman, M., Shekedef, M., Nada, A., and Ismail, A. (2017). *In vitro* and *in vivo* evaluation of tablets containing meloxicam-PEG 6000 ball-milled co-ground mixture. *J. Appl. Pharm. Sci.* 7 (3), 031–039. doi:10.7324/JAPS.2017.70306
- Fekete, T., Borsas, J., Takács, E., and Wojnárovits, L. (2016). Synthesis of cellulose-based superabsorbent hydrogels by high-energy irradiation in the presence of crosslinking agent. *Radiat. Phys. Chem.* 118, 114–119. doi:10.1016/j.radphyschem.2015.02.023
- Fernandes, G. J., Kumar, L., Sharma, K., Tunge, R., and Rathnanand, M. (2018). A review on solubility enhancement of carvedilol—a BCS class II drug. *J. Pharm. Innovation* 13 (3), 197–212. doi:10.1007/s12247-018-9319-z
- Ghosal, K., Adak, S., Agatemor, C., Kalarikkal, N., and Thomas, S. (2020). Novel interpenetrating polymeric network based microbeads for delivery of poorly water soluble drug. *J. Polym. Res.* 27 (4), 98. doi:10.1007/s10965-020-02077-6
- Ghosal, K., Ranjan, A., and Bhowmik, B. B. (2014). A novel vaginal drug delivery system: anti-HIV bioadhesive film containing abacavir. *J. Mater. Sci. Mater. Med.* 25 (7), 1679–1689. doi:10.1007/s10856-014-5204-6
- Homayun, B., Lin, X., and Choi, H.-J. (2019). Challenges and recent progress in oral drug delivery systems for biopharmaceuticals. *Pharmaceutics* 11 (3), 129. doi:10.3390/pharmaceutics11030129
- Hua, S. (2020). Advances in oral drug delivery for regional targeting in the gastrointestinal tract—Influence of physiological, pathophysiological and pharmaceutical factors. *Front. Pharmacol.* 11, 524. doi:10.3389/fphar.2020.00524
- Jana, S., Sharma, R., Maiti, S., and Sen, K. K. (2016). Interpenetrating hydrogels of O-carboxymethyl Tamarind gum and alginate for monitoring delivery of acyclovir. *Int. J. Biol. Macromol.* 92, 1034–1039. doi:10.1016/j.jbiomac.2016.08.017
- Jayaramudu, T., Raghavendra, G. M., Varaprasad, K., Reddy, G. V. S., Reddy, A. B., Sudhakar, K., et al. (2016). Preparation and characterization of poly(ethylene glycol) stabilized nano silver particles by a mechanochemical assisted ball mill process. *J. Appl. Polym. Sci.* 133 (7). doi:10.1002/app.43027
- Jermain, S. V., Brough, C., and Williams, R. O., III (2018). Amorphous solid dispersions and nanocrystal technologies for poorly water-soluble drug delivery—an update. *Int. J. Pharm.* 535 (1–2), 379–392. doi:10.1016/j.ijpharm.2017.10.051
- Kabanov, A. V., and Vinogradov, S. V. (2009). Nanogels as pharmaceutical carriers: finite networks of infinite capabilities. *Angew. Chem. Int. Ed.* 48 (30), 5418–5429. doi:10.1002/anie.200900441
- Khan, K. U., Minhas, M. U., Badshah, S. F., Sohail, M., and Sarfraz, R. M. (2022a). β -cyclodextrin modification by cross-linking polymerization as highly porous nanomatrices for olanzapine solubility improvement; synthesis, characterization and bio-compatibility evaluation. *J. Drug Deliv. Sci. Technol.* 67, 102952. doi:10.1016/j.jddst.2021.102952
- Khan, K. U., Minhas, M. U., Sohail, M., Badshah, S. F., Abdullah, O., Khan, S., et al. (2021). Synthesis of PEG-4000-co-poly (AMPS) nanogels by cross-linking polymerization as highly responsive networks for enhancement in meloxicam solubility. *Drug Dev. Industrial Pharm.* 47 (3), 465–476. doi:10.1080/03639045.2021.1892738
- Khan, K. U., Minhas, M. U., Syed, F. B., Suhail, M., Ahmad, A., Shakeel, I., et al. (2022b). Overview of nanoparticulate strategies for solubility enhancement of poorly soluble drugs. *Life Sci.* 291, 120301. doi:10.1016/j.lfs.2022.120301
- Khan, R., Zaman, M., Salawi, A., Khan, M. A., Iqbal, M. O., Riaz, R., et al. (2022c). Synthesis of chemically cross-linked pH-sensitive hydrogels for the sustained delivery of ezetimibe. *Gels* 8 (5), 281. doi:10.3390/gels8050281
- Mahmood, A., Ahmad, M., Sarfraz, R. M., and Minhas, M. U. (2016b). β -CD based hydrogel microparticulate system to improve the solubility of acyclovir: optimization through *in-vitro*, *in-vivo* and toxicological evaluation. *J. Drug Deliv. Sci. Technol.* 36, 75–88. doi:10.1016/j.jddst.2016.09.005
- Mahmood, A., Ahmad, M., Sarfraz, R. M., Minhas, M. U., and Yaqoob, A. (2016a). Formulation and *in vitro* evaluation of acyclovir loaded polymeric microparticles: a solubility enhancement study. *Acta Pol. Pharm.* 73, 1311–1324.
- Malik, N. S., Ahmad, M., and Minhas, M. U., Cross-linked β -cyclodextrin and carboxymethyl cellulose hydrogels for controlled drug delivery of acyclovir. *PLoS one*, 2017. 12(2): p. e0172727. doi:10.1371/journal.pone.0172727
- Martinez, M. N., and Amidon, G. L. (2002). A mechanistic approach to understanding the factors affecting drug absorption: a review of fundamentals. *J. Clin. Pharmacol.* 42 (6), 620–643. doi:10.1177/00970002042006005
- Nagra, U., Barkat, K., Ashraf, M. U., and Shabbir, M. (2022). Feasibility of enhancing skin permeability of acyclovir through sterile topical lyophilized wafer on self-dissolving microneedle-treated skin. *Dose-Response* 20 (2), 155932582210975. doi:10.1177/15593258221097594
- Nair, A. B., Attimmarad, M., Al-Dhubiab, B. E., Wadhwa, J., Harsha, S., and Ahmed, M. (2014). Enhanced oral bioavailability of acyclovir by inclusion complex using hydroxypropyl- β -cyclodextrin. *Drug Deliv.* 21 (7), 540–547. doi:10.3109/10717544.2013.853213
- Özkahraman, B., Acar, I., and Güçlü, G. (2022). Synthesis of N-vinylcaprolactam and methacrylic acid based hydrogels and investigation of drug release characteristics. *Polym. Bull.* 80, 5149–5181. doi:10.1007/s00289-022-04301-3
- Rafique, N., Ahmad, M., Minhas, M. U., Badshah, S. F., Malik, N. S., and Khan, K. U. (2022). Designing gelatin-based swellable hydrogels system for controlled delivery of salbutamol sulphate: characterization and toxicity evaluation. *Polym. Bull.* 79 (7), 4535–4561. doi:10.1007/s00289-021-03629-6
- Sadeghianmaryan, A., Karimi, Y., Naghieh, S., Alizadeh Sardroud, H., Gorji, M., and Chen, X. (2020a). Electrospinning of scaffolds from the polycaprolactone/polyurethane composite with graphene oxide for skin tissue engineering. *Appl. Biochem. Biotechnol.* 191 (2), 567–578. doi:10.1007/s12010-019-03192-x
- Sadeghianmaryan, A., Yazdanpanah, Z., Soltani, Y. A., Sardroud, H. A., Nasirtabrizi, M. H., and Chen, X. (2020b). Curcumin-loaded electrospun polycaprolactone/montmorillonite nanocomposite: wound dressing application with anti-bacterial and low cell toxicity properties. *J. Biomaterials Sci. Polym. Ed.* 31 (2), 169–187. doi:10.1080/09205063.2019.1680928
- Sarfraz, R. M., Ahmad, M., Mahmood, A., Akram, M. R., and Abrar, A. (2017). Development of β -cyclodextrin-based hydrogel microparticles for solubility enhancement of rosuvastatin: an *in vitro* and *in vivo* evaluation. *Drug Des. Dev. Ther.* Vol. 11, 3083–3096. doi:10.2147/dddt.s143712
- Shabir, F., Erum, A., Tulain, U. R., Hussain, M. A., Ahmad, M., and Akhter, F. (2017). Preparation and characterization of pH sensitive crosslinked Linseed polysaccharides-co-acrylic acid/methacrylic acid hydrogels for controlled delivery of ketoprofen. *Des. Monomers Polym.* 20 (1), 485–495. doi:10.1080/15685551.2017.1368116
- Sharma, M., Sharma, R., Jain, D. K., and Saraf, A. (2019). Enhancement of oral bioavailability of poorly water soluble carvedilol by chitosan nanoparticles: optimization

and pharmacokinetic study. *Int. J. Biol. Macromol.* 135, 246–260. doi:10.1016/j.ijbiomac.2019.05.162

Siddiqua, A., Ranjha, N. M., Rehman, S., Shoukat, H., Ramzan, N., and Sultana, H. (2022). Preparation and characterization of methylene bisacrylamide crosslinked pectin/acrylamide hydrogels. *Polym. Bull.* 79 (9), 7655–7677. doi:10.1007/s00289-021-03870-z

Tan, J., Luo, S., Ji, W., Li, Y., Li, L., and Cheng, X. (2022). Phase-changing hydrogels incorporated with copper sulfide-carbon nanotubes for smart thermal management and solar energy storage. *J. Energy Storage* 50, 104653. doi:10.1016/j.est.2022.104653

Uyanga, K. A., Okpozo, O. P., Onyekwere, O. S., and Daoud, W. A. (2020). Citric acid crosslinked natural bi-polymer-based composite hydrogels: effect of polymer ratio and beta-cyclodextrin on hydrogel microstructure. *React. Funct. Polym.* 154, 104682. doi:10.1016/j.reactfunctpolym.2020.104682

Wu, W., Huang, X., Li, K., Yao, R., Chen, R., and Zou, R. (2017). A functional form-stable phase change composite with high efficiency electro-to-thermal energy conversion. *Appl. Energy* 190, 474–480. doi:10.1016/j.apenergy.2016.12.159

Xie, Y., and Yao, Y. (2018). Octenylsuccinate hydroxypropyl phytylglycogen, a dendrimer-like biopolymer, solubilizes poorly water-soluble active pharmaceutical ingredients. *Carbohydr. Polym.* 180, 29–37. doi:10.1016/j.carbpol.2017.10.004

Zahir, M. H., Irshad, K., Aziz, M. A., Shafiqullah, M., Rahman, M. M., and Hossain, M. M. (2019). Shape-Stabilized phase change material for solar thermal energy storage: CaO containing MgCO₃ mixed with polyethylene glycol. *Energy and Fuels* 33 (11), 12041–12051. doi:10.1021/acs.energyfuels.9b02885

Zhou, X., Ling, K., Liu, M., Zhang, X., Ding, J., Dong, Y., et al. (2019). Targeted delivery of cisplatin-derived nanoprecursors via a biomimetic yeast microcapsule for tumor therapy by the oral route. *Theranostics* 9 (22), 6568–6586. doi:10.7150/thno.35353